atypia underwent immediate excision: 5/9 (56%) were benign, 1/9 (11%) had atypical ductal hyperplasia and 3/9 (33%) had invasive carcinoma (pure mucinous or mucinous features). Overall, a total of 4/32 (13%) cases of MLL were upgraded to carcinoma, 3 of which were initially diagnosed on ultrasound core biopsies.
Conclusions: None of the patients in this series with benign MLL on core biopsy had invasive carcinoma on excision. However, 16% had atypical ductal hyperplasia and 5% had ductal carcinoma in situ. Patients with MLL and atypical ductal hyperplasia or detached atypical cells on core biopsy were more likely to have invasive carcinoma on excision. These findings suggest that core biopsy findings may identify patients at the highest risk for upgrade to carcinoma on excision but validation in larger studies is required.

311 Expression Analysis of Epithelial-Mesenchymal Transition Related Genes in Triple Negative Breast Cancer

Shuling Zhou, Anqi Li, Ming Li, Yan Xu, Yaoxing Xiao, Wentao Yang. Fudan University Shanghai Cancer Center, Shanghai, China.
Background: Triple negative breast cancer (TNBC) is a group of highly heterogeneous tumor. 6 subtypes were identified in TNBC, including basal-like 1, basal-like 2, immunomodulatory (IM), mesenchymal (M), mesenchymal stem–like (MSL), and luminal androgen receptor (LAR). M and MSL subtypes were closely related with epithelial mesenchymal transition (EMT).
Design: 179 cases of TNBC who underwent surgery in Fudan University Cancer Hospital were collected, including 145 cases of invasive carcinoma of no special type (ICONST), 12 cases of squamous cell carcinoma (SCC), 14 cases of spindle cell carcinoma (SpCC) and 8 cases of matrix producing carcinoma (MPC). Expression of EMT related genes (E-cadherin, slug, twist and vimentin) were dectected by immunohistochemistry in TNBC tissue array.
Results: 124 cases (124/179, 69.3%) were E-cadherin positive. Positive rate of E-cadherin in ICONST, SCC, SpCC and MPC patients were 78.6% (114/145), 83.3%(10/12), 0.0%(0/14) and 0.0%(0/8). The expression was significantly higher in ICONST and SCC patients than in that of SpCC and MPC patients (P<0.0001). 51 cases (51/179, 28.5%) were slug positive. Positive rate of slug in ICONST, SCC, SpCC and MPC patients were 19.4%(28/145), 33.3%(4/12), 78.6%(11/14), 100.0%(8/8) respectively. The expression of slug was significantly higher in SpCC and MPC patients than that in ICONST and SCC patients (P<0.05). 83 cases (83/179, 46.4%) were twist positive. Positive rate of slug in ICONST, SCC, SpCC and MPC patients were 19.4%(28/145), 33.3%(4/12), 78.6%(11/14), 100.0%(8/8), respectively. The expression was significantly higher in SpCC and MPC patients than that in ICONST and SCC patients (P<0.05). 67 cases (67/179, 37.4%) were vimentin positive. Positive rate of vimentin in ICONST, SCC, SpCC and MPC patients were 30.3%(44/145), 8.3%(1/12), 100.0%(14/14), 100.0%(8/8). The expression was significantly higher in SpCC and MPC patients than that in ICONST and SCC patients (P<0.0001). The expression of Slug and Twist were negatively correlated with the expression of E-cadherin, while positively correlated with vimentin expression (P<0.05).
Conclusions: SpCC and MPC patients displayed lower expression of epithelial marker (E-cadherin), higher expression of EMT-related transcription factors (slug, twist) and mesenchymal marker (vimentin), which indicated the role of EMT in MPC and SpCC. Slug and twist may regulate the expression of vimentin and downregulate the expression of E-cadherin in TNBC.

312 Droplet Digital Polymerase Chain Reaction Detection of HER2 Amplification in Formalin Fixed Paraffin Embedded Breast and Gastric Carcinoma Samples

Ya-Zhen Zhu, Dan Lu, Maruja E Lira, Qing Xu, Yunzhi Du, Jianghong Xiong, Mao Mao, Hyun Cheol Chung, Guangjuan Zheng. Guangdong Provincial Hospital of Traditional Chinese Medicine (GPHTCM), Guangzhou, China; WuXi AppTec, Shanghai, China; Pfizer Oncology, San Diego, CA; Yonsei University College of Medicine, Seoul, Korea.
Background: Human epidermal growth factor receptor 2 (HER2) is a key driver of tumorigenesis, and over-expression as a result of HER2 gene amplification has been observed in a number of solid tumors. Recently HER2 has become an important biomarker for the monoclonal antibody treatment of HER2-positive metastatic breast and advanced gastric cancer. The HER2 targeting antibody Trastuzumab treatment requires accurate measurement of HER2 levels for proper diagnosis. Droplet digital PCR (ddPCR) with highly direct, precise and absolute nucleic acid quantification could be used to detect HER2 amplification levels. The aim of the present study was to evaluate a robust, accurate and less subjective application of ddPCR for HER2 amplification levels and test the assay performance in clinical formalin-fixed paraffin-embedded (FFPE) breast and gastric carcinoma samples.
Design: Genomic DNA from HER2 amplified cell line SK-BR-3 was used to set up the ddPCR assays. The copy number of HER2 was compared to the chromosome 17 centromere reference gene (CEP17), expressed as HER2:CEP17 ratio. Genomic DNAs of FFPE specimens from 145 Asian patients with breast and gastric carcinomas were assayed using both standard methods, immunohistochemistry (IHC) and/or fluorescence in situ hybridization (FISH), and ddPCR.
Results: Based on 145 clinical breast and gastric carcinoma cases, our study demonstrated a high concordance of ddPCR results to FISH and IHC. In breast cancer specimens, the ddPCR results had high concordance with FISH and IHC defined HER2 status with a sensitivity of 90.9% (30/33) and a specificity of 100% (77/77). In gastric cancer specimens that were concordant in both FISH and IHC, our assay was 95.5% concordant with FISH and IHC (21/22).
Conclusions: ddPCR has the advantage of automation and also allows levels of HER2 amplification to be easily evaluated in large numbers of samples, and presents a potential option to define HER2 status.

Cardiovascular Pathology

313 Unusual Complications of Prosthetic Vascular Reconstruction: A Clinicopathologic Case Series

Ibrahim Aboshady, Naveed U Saqib, Deborah Vela, Ana M Segura, Kamal Khalil, L Maximilian Buja. Texas Heart Institute, Houston, TX; The University of Texas HSC, Houston, TX.
Background: Typical complications of vascular reconstructive surgery are thrombosis, infection pseudoaneurysm, dilation, and AE fistula/erosion. Certain, rarer complications are often ignored, unforeseen, or misinterpreted during surgery.
Design: We report 5 cases. Patient 1, a 72-year-old woman, died of an invasive intimal angiosarcoma (AS) detected in a 4.5-cm TAAA during surgical repair. Patients 2 and 3 had a superficial spreading intimal AS detected during replacement of Dacron-coated grafts implanted 5 and 9 years earlier. Patient 4, a 61-year-old woman who had undergone aortic repair, died of consequent acute severe bacterial meningitis involving the hippocampal region, choroid plexus, and pituitary gland. Patient 5 had a spinal cord infarct after undergoing open repair of inflammatory AAA.
Results: In the 3 AS cases, we studied—and sought therapeutic targets in—selective molecular pathways that may be involved in the transformation of benign to malignant endothelium. The proteins Akt/mTOR, STAT 3, COX-2, and CD44 were expressed in all lesions. H&E staining showed thickened intima with calcified atherosclerotic lesions, and elastin staining showed diminished elastin fiber, medial degeneration, high-grade sarcoma, high N/C ratio, numerous atypical mitoses, and large areas of tumor necrosis. IHC results were strongly positive for vimentin, focally and unevenly positive for CD 31, and negative for pancytokeratin, CK-7, CK-20, calretinin, D-2-40, CD-45, S-100, MA, and CD 34; 95% of tumor cells were positive for Ki-67. The meningitis patient was anxious, tachypneic, hypothermic, paraplegic, and leukopenic (3.1k/cmm) after aortic repair. CSF showed RBC 96,250, WBC 4100 (93% PMN), glucose <1, protein 584, and visible gram-negative rods. MRI showed small left cerebellar and intraventricular hemorrhage; CSF, blood, and urine cultures grew *Klebsiella pneumoniae*.
Conclusions: These cases contribute to the body of knowledge regarding these unusual perioperative proximal and distal complications, whether immediate or delayed, helping reveal the spectrum of disease that may arise in vasculature tissues, either spontaneously or after synthetic-graft placement. To manage these unusual complications properly, surgeons should take timely and adequate biopsies from any ***ambiguous*** vascular reconstructive lesions for histopathologic study.

314 Regional Differences in Ascending Aortic Histology: A Comparative Histomorphologic Assessment with Implication for Pathologic Classification

Md Shahrier Amin, Cecilia Wu, Charles Leduc, Peter T Lin, Sarah M Jenkins, William D Edwards, Joseph J Maleszewski. Mayo Clinic, Rochester, MN.
Background: The aortic sinuses (AS) are often involved in cases of aneurysm and/or dissection. In contrast to the tubular aorta (TA), the histomorphologic features of the AS have yet to be systematically characterized, which can potentially lead to diagnostic misinterpretation. Accurate knowledge of regional variations in aortic histomorphology is also useful in the design of prosthetic biomaterials. The aim of this study was to determine the range of histomorphologic features, in the normal AS across a broad age range.
Design: Autopsy-derived ascending aortic specimens were prospectively collected over a 1-year period. Decedents with a history of significant cardiovascular disease were excluded. Transverse sections of the AS and TA were collected and stained with H&E and VVG. The following parameters were blindly evaluated by 3 pathologists: medial thickness, elastic tissue amount, lamellar units per 200X field, pattern of major elastic fibers (parallel or woven) and intralamellar distance. Measures were compared between AS and TA with paired t-test. Linear regression was used for comparisons with age.
Results: 32 cases (17 women, mean age 56.9 years, range 12-85; 15 men, mean age 62 years, range 13-90) met inclusion criteria. The media was significantly thicker in the TA (1215±213 mm) vs. the AS (879±249 mm) (p<0.0001). While there was no difference in the quantity of elastin, there were significantly more lamellar units in the TA (29±5) vs AS (25±5) (p<0.0001) with smaller intralamellar distance (TA 21.4±4.2 mm vs AS 23.4±4.6 mm) (p=0.0006). A woven pattern of elastic fibers was more commonly identified in the AS (93.8%), while a parallel pattern was more commonly identified in the TA (90.6%) (p<0.0001). Ratio of media thickness between AS to TA decreased with age (p=0.04), as did the distance between elastic fibers in the AS only (p=0.003) and not in the TA.
Conclusions: This is the first study to systematically and comparatively evaluate the histomorphology of the AS across a broad age range. The results highlight the unique histomorphometric features of the AS, that can mimic medial degenerative changes and lead to mischaracterization. This underscores the importance of proper orientation and sampling of surgically resected aortas. Examination for region-specific pathologies in various disease states is ongoing. While the functional significance is not yet clear, the decrease in AS intralamellar elastic fiber distance with age might contribute to the age-associated increase in aortic root diameter.

315 Repair of the Injured Adult Heart Involves Regionally Specific c-Kit+ Cardiac Stem Cells and New Myocyte Formation

David Angert, Remus Berretta, Hajime Kubo, Tim Starosta, Daniel Luthringer, Steven R Houser. Cedars-Sinai Medical Center, Los Angeles, CA; Temple University School of Medicine, Philadelphia, PA.

Background: Cardiac injury induces persistent sympathetic activity that causes myocyte death. We studied cardiac injury, elicited via excess catecholamines, in an animal model, & assessed regional specificity of new myocyte generation from c-kit+ cardiac progenitor cells (CPCs). In the human heart, we identified and compared c-kit+ regional specificity.

Design: Cardiomyopathy was induced in adult felines by infusion of Isoproterenol (ISO) for 10 days. Animals were studied at Day 10 (D10; injury), 17 & 38. Bromodeoxyuridine (BrdU; proliferative cells) was infused 7 days prior to explant (D10, 17 or 38), OR (for Pulse-Chase) through Day 10, removed, & tissue examined after recovery (D38). In human hearts, regional specificity of c-kit+ cells was studied in heart failure (HF) vs control (Con) hearts.

Results: The model showed that ISO significantly decreased (↓) ejection fraction (EF), with a significant increase (↑) in % collagen. By D17, post ISO, EF recovered. At D10 (injury) there was a ↑ in BrdU+ nuclei in the LV but few BrdU+ myocytes. A significant ↑ in the % of c-kit+ & c-kit+BrdU+ nuclei were found at Day 10 vs Con, in the Apex (c-kit+ 0.34±0.04; c-kit+BrdU+ 0.09±0.01, $p<0.001$) vs Mid & Base, & Epicardium (Epi) (c-kit+ 0.43±0.02; c-kit+BrdU+ 0.25±0.02, $p<0.001$) vs Mid-Myocardium & Endocardium (Endo) of the heart. However, at D17, there were ↑ BrdU+ myocytes in the Apex (0.22±0.04, $p<0.001$) & Epi (0.20±0.05, $p<0.001$). Our most provocative finding was the ↑ in BrdU+ myocytes in the Apex & Epi at D38 (Chase) when BrdU was infused during injury (Pulse; through D10), supporting the data that ↑ c-kit+ & c-kit+BrdU+ CPC's from D10, in the Apex & Epi, are a contributor to new myocytes. Consistent in the human heart, ↑ c-kit+ cells were found in HF vs Con. In the LV, c-kit+ cells were ↑ in the Apex (0.27±0.06, $p<0.001$) & Epi (0.30±0.06, $p<0.001$). In the left & right atria, c-kit+ cells were ↑ in the Epi, & interestingly, in the Endo.

Conclusions: Catecholamine injury induces a regionally specific increase of c-kit+ CPC's, in animal model & human. Importantly, when ISO was reduced, BrdU+ myocytes at D17 & D38 were greater in the Apex & Epi, likely in part from ↑ c-kit+ CPC's labeled during injury phase (D10). The regional specificity of c-kit+ cells in human HF is consistent with these findings, with the unique observation that ↑ c-kit+ cells are present in both the Epi & Endo of the atria.

316 Human Plaque-Aortic Ring Co-Culture: A Novel Assay for the Study of Atherosclerosis-Induced Angiogenesis

Alfred C Aplin, Ted Kohler, Roberto Nicosia. University of Washington, Seattle, WA; VA Puget Sound HCS, Seattle, WA.

Background: Atherosclerosis is a major cause of morbidity and mortality worldwide. Progression of atherosclerotic plaques into vulnerable lesions is often associated with angiogenesis which contributes to plaque growth, inflammation and hemorrhage. Although angiogenesis is recognized as an important contributor to the complications of atherosclerosis, the mechanisms of plaque-induced angiogenesis are poorly understood. Lack of adequate experimental models has significantly limited progress in this field.

Design: Human plaques obtained from carotid endarterectomy or leg amputation procedures were co-cultured in collagen gels with rings of rat aorta which served as read-out of plaque angiogenic activity. Angiogenesis was quantified by counting microvessels sprouted from aortic rings over time. The cellular composition of the outgrowths was evaluated by immunohistochemistry. The growth factor/cytokine secretome of human plaques was analyzed by immunochemistry. Antibody blocking experiments were used to define the role of plaque-derived growth factors in the angiogenic response.

Results: Human plaque explants cultured alone failed to produce an angiogenic response except for isolated endothelial sprouts in rare explants. However when co-cultured with rat aortic rings, plaque explants markedly stimulated angiogenesis from the aortic wall. The angiogenic outgrowth was composed of endothelial cells, pericytes, macrophages and mesenchymal cells. Analysis of the plaque secretome demonstrated heterogeneity of growth factor/cytokine production by different plaques. Blocking antibody experiments showed that targeting of individual growth factors such as vascular endothelial growth factor or tumor necrosis factor alpha failed to effectively suppress angiogenesis. Conversely ablation of adventitial macrophages from the aortic rings markedly reduced the angiogenic response.

Conclusions: Human atherosclerosis-induced angiogenesis can be studied ex vivo by co-culturing plaque explants with rat aortic rings. Our results suggest that human plaque-induced angiogenesis is regulated by a redundant system of growth factors and cytokines and significantly influenced by adventitial macrophages. This model may prove useful to identify molecular pathways that initiate angiogenesis which can be targeted pharmacologically toward the goal of stabilizing atherosclerotic plaques and preventing the life-threatening complications of atherosclerosis.

317 Unique Insights into Cardiac Metastases and Tumor Biology from a Cancer Center's Rapid Research Autopsy Program

Prashant Bavi, Hamidreza Sharifzad, Qian Yang, Leslie Oldfield, Anthony Joshua, Jagdish Butany, Michael H Roehrl. University Health Network, Toronto, ON, Canada; Memorial Sloan Kettering Cancer Center, New York, NY.

Background: Targeted therapies may be inducing selection pressure where unique tumor clones evolve with a propensity for unusual clinical presentation like cardiac metastases. Metastases to the heart are far more common than primary cardiac tumors. Here, we study cardiac metastases from our comprehensive rapid research autopsy program.

Design: 105 patients who had consented to undergo directed rapid ("warm") autopsies have been studied. We investigated the extent of metastatic spread with an emphasis on cardiac metastases by focusing on the following aspects: (1) Tumor kinetics by integrating radiographic imaging findings and tumor burden; (2) number of metastases, size, and location; (3) clinical symptoms; (4) genome sequencing, transcriptomics, and proteomics of selected cases.

Results: The incidence of cardiac metastases in our cohort was 21.9% (23/105), significantly higher than previous reports. Patient age ranged from 25 to 86 years (median, 64 years); gender distributions was 15 males and 9 females; histology: 13 carcinomas (GI and lung mostly), 6 melanomas, 3 leukemias/lymphomas, and 1 sarcoma. The weight of the heart ranged from 180 to 560 g (median, 335 g); size of cardiac metastases ranged from 0.3 to 40 mm (median, 5 mm) and number of metastases: solitary (n=5) and multiple (n=18). The median time from last imaging to autopsy was 36.5 days (25%-75% IQR, 20.7-76.0). There was significant underestimation of cardiac metastases at last radiologic imaging in virtually all patients; only two had documented cardiac lesions at imaging. Of these 23 patients, 8 (33.7%) were on clinical trial, 14(60.8%) received chemotherapy and or radiation, and 2 (8.6%) did not receive any treatment. Whole genome sequencing, RNASeq, and mass spec proteomics have been carried out successfully on all metastatic tumor sites from 2 rapid autopsy cases. Comparative whole genomes/exomes, RNAseq, and proteomics from multiple metastatic sites in pancreatic cancer showed that heart metastases clustered as distinct entities on a Jensen-Shannon (JS) dendogram.

Conclusions: (1) A very high incidence of cardiac metastases was observed.
(2) Cardiac metastases were molecularly distinct from other solid organ metastases.
(3) Underestimation of cardiac metastases by radiology is common.
(4) With expected continued therapeutic improvements, metastases to the heart if not diagnosed and treated, may prove to be a limiting factor in improving long-term survival.

318 Clinicopathologic Experience with Mitral Valve Repairs Using CorMatrix ECM® Technology

Siddharth Bhattacharyya, Shiguang Liu, Nirag Jhala, He Wang. Temple University Hospital, Philadelphia, PA.

Background: Mitral regurgitation is a common complication of myocardial infarction, and is associated with significant mortality and morbidity. Clinical evidence suggests that mitral valve repair has advantages over mitral valve replacement in both morbidity and mortality reduction. Newer options for repair include the use of artificial biomaterials. CorMatrix is an organic and acellular extracellular matrix, which is harvested from porcine small bowel submucosa. CorMatrix acts as a tissue scaffold, and is intended to promote neo-vascularization and remodeling to replicate normal tissue function. Early studies have found CorMatrix to be suitable for mitral valve repair, with excellent valvular function post-operatively. Our purpose is to present data on our institutional experience with the use of CorMatrix for mitral valve repair.

Design: At our institution in 2013-2014, CorMatrix material was utilized during mitral valve repair surgery for eight patients with severe mitral regurgitation. The patient group consisted of two males and six females, ages ranging from 34 to 78 years. One patient had a history of rheumatic heart disease, and the remaining patients had histories of hypertension among other comorbidities. Four patients eventually developed recurrent mitral valve regurgitation requiring repeat intervention, and in some cases valve replacement. The time to graft failure ranged from 4-14 months. Native valve tissue and graft sections were submitted for histologic examination.

Results: Histologic examination in all cases showed acellular graft material associated with a moderate to marked lymphoplasmacytic inflammatory infiltrate with focal acute inflammation and fibrinoid necrosis. Two cases showed marked granulomatous inflammation with multinucleated giant cells. Focal areas of fibroblastic proliferation and neo-vascularization were noted. However, no evidence of new intimal formation or remodeling was seen in any case. Immunohistochemical staining for CD68 and CD163 showed a predominant M1 macrophage phenotype, consistent with a pro-inflammatory response.

Conclusions: While our sample size is small, our clinical experience shows a failure rate of 50% when using CorMatrix for mitral valve repair. Graft failure in each cases occurred between 4-14 months. Histologic sections of graft material show significant chronic inflammation with no evidence of remodeling. Our evidence suggests that CorMatrix is not a suitable material for mitral valve grafts.

319 Apolipoprotein A-IV Associated Cardiac Amyloidosis

Melanie C Bois, Surendra Dasari, Jason D Theis, Julie Vrana, Martha Grogan, Angela Dispenzieri, Paul J Kurtin, Joseph J Maleszewski. Mayo Clinic, Rochester, MN.

Background: Apolipoprotein A-IV (Apo AIV) is known to co-deposit with other amyloid subtypes, and has been found to be the primary constituent in some cases of renal amyloidosis. However, cases of cardiac amyloidosis solely attributable to Apo AIV amyloid (AApoAIV) have not been described. Herein, we describe clinical and histopathological characteristics of cardiac AApoAIV, a novel type of cardiac amyloid.

Design: Tissue registry archives at Mayo Clinic (Rochester, Minnesota) were queried for cases of cardiac amyloidosis typed as AApoA4 by liquid chromatography tandem mass spectrometry (2006-2015). Extent and pattern of amyloid deposition were assessed. Dominant and coexisting deposition patterns were classified as vascular (obstructive or non-obstructive), interstitial (nodular, discrete pericellular, or dispersed pericellular), and endocardial. Salient clinical information, epidemiological data, and imaging features were abstracted from the clinical record.

Results: 12 patients (pts; 10 men) with cardiac AApoA4 were identified with a mean age of 75 years (range, 64-89). 4 autopsy cases and 4 surgical specimens (total=8) were available for histopathologic and clinical review; 4 consultation cases had epidemiologic information only. 7 of 8 patients had symptomatic cardiac dysfunction, 4 of which carried a diagnosis of hypertrophic cardiomyopathy and 3 were attributed to coronary artery disease. 6 pts had conduction system abnormalities. Left ventricular ejection fraction was preserved in the 7 cases with echocardiographic data (median 59%, IQR 54-67%).

7 pts had renal insufficiency. Of available cases (n=8), the dominant deposition pattern was vascular in 4 cases and nodular interstitial in 4. Amyloid extent was marked in 2 cases, moderate in 4, and mild in 2 cases. Obstructive vascular amyloid and interstitial involvement were present in all cases. 3 cases had focal endocardial involvement. All autopsy cases demonstrated small vessel involvement in other visceral organs and prominent medullary renal deposits.

Conclusions: AApoAIV is a rare, novel subtype of cardiac amyloidosis. Vascular tropism and relatively large nodular interstitial deposits appears to be common histopathologic features of cardiac AApoAIV. Atypical clinical presentations, where amyloid was not a primary diagnostic consideration, are present in at least half of the cases. Limited autopsy experience suggests relatively widespread vascular involvement in most organs systems and renal medullary deposits in the setting of AApoAIV amyloidosis. Molecular genetic analysis of the *ApoAIV* gene in a select group of these patients is ongoing.

320 Endothelial Cell Chimerism in Human Cardiac Allografts

Gregory A Fishbein, Maristela L Onozato, Adriana Luk, Michael M Givertz, Robert F Padera, Jr., Anthony J Iafrate, Richard N Mitchell. Brigham and Women's Hospital, Boston, MA; Massachusetts General Hospital, Boston, MA.

Background: It is unknown to what degree circulating endothelial cells (CEC) replace donor endothelium in cardiac allografts; perioperative ischemic injury or rejection may increase this potential. Moreover, as endothelial cells are the interface between the host immune system and the allograft, replacement of donor endothelium may protect against acute cellular rejection (ACR) and/or antibody-mediated rejection (AMR).

Design: Thirty-nine endomyocardial biopsies of 12 male recipients of female hearts, performed at 1, 3, 6, and 12 months post-orthotopic heart transplant (OHT) were evaluated for ACR and AMR by one of three pathologists. Endothelial cells were segregated as donor or recipient based on detection of X and Y chromosomes by fluorescence *in situ* hybridization. Endothelial cells were identified by positive fluorescent immunoreactivity to CD34 antigen and negative reactivity to CD45 antigen; such cells exhibiting two X chromosomes were designated as donor, while those with one X and one Y chromosome were designated as recipient.

Results: An average of 103 endothelial cells per biopsy were analyzed. Endothelial cell chimerism, defined as the percentage of endothelial cells with X and Y chromosomes, at 1, 3, 6, and 12 months post-OHT can be seen in figure 1.

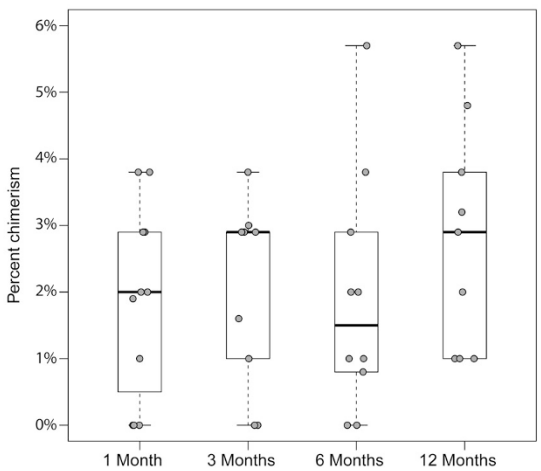

Over the 12 months, all subjects had at least one biopsy showing mild or moderate ACR (ISHLT 1R or 2R); three had at least one episode of pathologic AMR. Seven subjects showed an overall increase in chimerism over time, one of whom developed AMR. Five showed an overall decrease, two of whom developed AMR. Three subjects showed no chimerism 1 month following OHT; all three had at least one episode of moderate ACR; one had multiple biopsies positive for AMR. All biopsies following episodes of rejection showed an increase in chimerism.

Conclusions: Our data indicate that within one month post-OHT the average chimerism is 1.9% (0-3.9%). Six months post-OHT, up to 6% of donor endothelial cells were replaced by CEC of recipient origin. This number increases following episodes of ACR. Most individuals showed an increase in chimerism over time. AMR was more common in the minority of individuals who experienced decreasing chimerism over time, suggesting that replacement of donor endothelial cells may be protective.

321 NRG1-ERBB4-PSEN1 Dysfunction in Human Myocarditis and Dilated Cardiomyopathy

Paul J Hanson, Erika L Jang, Angela Y Chang, Harpreet Rai, Angela Y Mo, Bruce M McManus, Michael A Seidman. University of British Columbia, Vancouver, BC, Canada; Providence Health Care, Vancouver, BC, Canada.

Background: Myocarditis, inflammation of the heart muscle, may be caused by infection (most often viral), autoimmunity, or chemical exposure. Clinical symptoms are also variable, with some patients, regardless of etiology, experiencing life threatening acute illness, others suffering from chronic disease, and still others who never present clinically. The risk factors for developing different patterns of disease are poorly elucidated, but preclinical and limited clinical studies have implicated a role for the signalling cascade involving neuregulin 1 (NRG1), epidermal growth factor related receptor ERBB4, and presenilin 1 (PSEN1). This study aims to characterize the same signalling pathway in archival human tissue specimens from patients with a diagnosis of myocarditis. Therefore it's hypothesized that variable expression and function of the NRG1-ERBB4-PSEN1 signaling axis are associated with different clinical manifestations of myocarditis.

Design: Nine (9) cases of myocarditis and one (1) normal control were identified from the Cardiovascular Tissue Registry in the Centre for Heart Lung Innovation. Using archival tissue from the left ventricle of each case, protein expression levels, cellular localization, and post-translational modifications of NRG1, ERBB4, and PSEN1 were evaluated using immunohistochemistry, immunofluorescence, and western blotting.

Results: NRG1, ERBB4, and PSEN1 were expressed at higher levels in the majority of myocarditis cases compared to the normal heart tissue. All three proteins accumulated in the nucleus of myocarditis hearts, while PSEN1 was also detected in extracellular protein aggregates (plaques) in myocarditis cases, while ERBB4 also accumulated in lysosomes. ERBB4 and PSEN1 were found to co-localize in and out of the nucleus. Western blots showed NRG1 as 50 kDa, ERBB4 showed 80 and 120 kDa cleavage products, PSEN1 was detected as a 47 kDa holoprotein, as well as two PSEN1 aggregates approximately 100 kDa and between 47 and 75 kDa ranges.

Conclusions: Preliminary studies show a distinct difference in expression patterns of NRG1, ERBB4, and PSEN1 in cases of myocarditis as compared to normal heart controls. Further experiments are likely to establish patterns of expression that correlate with disease severity and temporality. These data may provide diagnostic and therapeutic guidance with respect to the different clinical manifestations of myocarditis.

322 Long Term Durability of Edwards SAPIEN Transcatheter Aortic Valves: A Pathology Study

Elena Ladich, Kazuyuki Yahagi, Robert Kutys, Michelle Olson, Renu Virmani. CVPath Institute, Gaithersburg, MD.

Background: Surgical bioprosthetic aortic valves (SAV) offer many advantages to patients with aortic stenosis but pathologic studies have reported limited durability of these devices due to calcific and non-calcific deterioration over time. The long-term pathological changes observed in Edwards SAPIEN transcatheter aortic valve (ESTAV) following implantation have not been well characterized.

Design: From our ESTAV pathology registry, 29 cases (mean age 82.6±7.9 years, 52% men) with ESTAV were included, which were removed either at autopsy or surgery. Valve leaflets were embedded in paraffin and stained with hematoxylin and eosin (HE), Movat's pentachrome (MO) and Von Kossa (VK). Neointima, thrombus, inflammation, structural changes (degeneration), and calcification of leaflets were evaluated histologically and semi-quantitatively graded for both aortic and ventricular surfaces of the leaflet (Score 0-4). Pathological findings were assessed by duration (≤30 days; 31 days-1 years; 1-3 years; >3 years) of implant.

Results: The mean implant duration was 210±500 days. The majority of patients had valves implanted ≤30 days; 5 valves were implanted > 3 years (≤30 days=20[69%]; 31 days-1 years=4 [14%]; 1-3 years=0[0%]; >3 years=5[17%]). Of 29 patients, there were single ESTAV (n=21), ESTAV-in-ESTAV (n=5), and ESTAV-in-SAV (n=3). Neointima and leaflet degeneration increased over time but were mild even > 3 years (neointima; ≤30 days: 0.02±0.08, 31 days-1 years: 0.13±0.10, >3 years: 0.77±0.09, P<0.0001; degeneration; ≤30 days: 0.02±0.04, 31 days-1 years: 0.11±0.13, >3 years: 0.48±0.49, P=0.0004). Inflammation and thrombus scores did not differ significantly over time and were generally mild (Thrombus; ≤30 days: 0.87±0.54, 31 days-1 years: 0.97±0.61, >3 years: 0.71±0.32, P=0.75, Inflammation; ≤30 days: 0.79±0.68, 31 days-1 years: 1.21±0.71, >3 years: 0.98±0.29, P=0.47). Calcification was observed in two valves > 3 years: one valve (4 years) showed early microcalcifications at a leaflet commissure; a second valve was explanted for aortic stenosis due to calcification at 5 years post implantation.

Conclusions: All explanted valves demonstrated intact leaflets with mild inflammation, thrombus and neointima up to 5 years. Degeneration was minimal and stenosis due to calcification was seen in one valve at 5 years, a complication also reported in SAV of similar duration. The pattern of calcification in ESTAV recapitulated that reported for SAV with early microcalcifications found predominately at commissures (region of high stress). Overall, valve leaflet durability for ESTAV appears to be comparable to SAV.

323 Neoatherosclerosis as a Cause of Late Stent Failure Following Bare Metal and 1st- and 2nd-Generation Drug-Eluting Stent Placement: An Autopsy Study

Elena Ladich, Maria Romero, Fumiyumi Otsuka, Renu Virmani. CVPath Institute, Gaithersburg, MD.

Background: In-stent neoatherosclerosis has emerged as an important contributing factor for late stent failure including very late stent thrombosis (VLST) and restenosis. The aim of the current pathologic study was to investigate the prevalence of neoatherosclerosis in lesions with late stent failure following bare metal (BMS) and 1st- and 2nd-generation (gen) drug-eluting stent (DES) placement.

Design: All stents from our autopsy stent registry with implant duration >30 days to include a total of 384 cases (mean age=61±13 years, 287 male) with 614 stented lesions in native coronary arteries (BMS=266 [median, 832 days], 1st-gen DES=285 [383 days], and 2nd-gen DES=63 lesions [210 days]) were evaluated for the involvement of neoatherosclerosis in stent thrombosis and restenosis.

Results: The prevalence of VLST (>1 year) was greater in 1st-gen DES (19%) as compared with BMS (3%) and 2nd-gen DES (0%), where in-stent plaque rupture from neoatherosclerosis accounted for 83% of VLST in BMS (5 of 6) and 15% of VLST in 1st-gen DES (5 of 33). The involvement of neoatherosclerosis in VLST increased with time; for duration of implants >3 years, all VLST in BMS (5 of 5) and 33% of VLST in 1st-gen DES (4 of 12) were attributed to in-stent rupture. VLST from in-stent rupture occurred earlier in 1st-gen DES (1434±579 days) vs. BMS (2376±545 days). Of the 10

lesions with in-stent rupture, only 4 (BMS=3, 1st-gen DES=1) had in-stent restenosis. In BMS, restenosis with underlying neoatherosclerosis was observed only >3 years, and neoatherosclerosis accounted for 38% of BMS restenosis >3 years. In contrast, both 1st- and 2nd-gen DES showed restenosis with neoatherosclerosis even ≤1 year. While only limited cases were available for 2nd-gen DES >1 year, 1st-gen DES showed increased involvement of neoatherosclerosis in restenosis over time, accounting for 31% of restenosis between 1 and 3 years and 78% of restenosis >3 years.
Conclusions: Neoatherosclerosis in late stent failure is observed in both BMS and DES, which increases over time.

324 Evaluation For Heritable Cardiovascular Disorders Using Targeted Next-Generation Sequencing on Formalin-Fixed Paraffin Embedded Tissue

Charles Leduc, Laura J Train, Rajeswari Avula, Katrina E Kotzer, Michelle L Kluge, Michael J Ackerman, Linnea M Baudhuin, Joseph J Maleszewski. Mayo Clinic, Rochester, MN.
Background: Heritable cardiovascular (CV) disorders are diverse and include channelopathies (CP), cardiomyopathies (CM) and connective tissue disorders (CTD). Because they are associated with catastrophic CV events, identification of those at-risk is paramount. While a strong family history can prompt screening, post-mortem genetic testing is often lacking. Furthermore, ideal specimens (i.e. whole blood (WB)) often are note retained at autopsy. Ubiquitous use of formalin-fixed paraffin embedded tissue (FFPET) in autopsy makes it an ideal source for interrogation; however its use in traditional sequencing is limited owing to genomic integrity. Targeted next generation sequencing (NGS) technology offers the ability to circumvent such limitations. The primary aim was to evaluate the efficacy of testing FFPET for heritable CV disorders using NGS.
Design: Paired FFPET (heart) and blood (WB or dried blood spot (DBS)) samples were obtained from 13 patients. 7 were random autopsy samples, 3 were autopsies with clinical phenotype of a heritable CV disorder but unknown genotype, and 3 were surgical samples from patients with genotype-confirmed hypertrophic cardiomyopathy (HCM) on blood. Extracted genomic DNA underwent Agilent SureSelect targeted capture of 101 genes associated with CP, CM, and CTD, followed by sequencing on the Illumina MiSeq. Quality metrics were compared. Variants were classified by consensus.
Results: In quality comparisons of 10 cases using the CM discovery panel (63 genes), there were no significant differences between FFPET, WB and DBS in average percent mapped reads (60 vs 55 vs 60%), average depth of coverage (1259 vs 1425 vs 1490X), and Phred quality scores (all >30). Analysis of surgically derived FFPET from HCM patients, confirmed pathogenic mutations in *TPM1*, *MYH7*, and *MYBC3*, previously detected on WB. In the 3 autopsy cases with unknown genotype, testing on FFPET identified pathogenic mutations in *FBN1*, *RAF1*, and *MYBC3,* consistent with the clinical phenotype of Marfan syndrome, Noonan syndrome, and HCM, respectively. There was 100% concordance for all genotype calls, with no false positives or false negatives.
Conclusions: The results of this validation study show similar performance characteristics for NGS of DNA derived from FFPET (≤17 years old), WB, and DBS, in the evaluation of inherited CV disorders. Such has important implications for molecular genetic testing when only FFPET is available. Additionally, interrogation of such tissues has important implications for extensive genotype-phenotype correlation in archival tissue, which is currently ongoing.

325 Cardiac Angiosarcoma: Histopathologic, Immunohistochemical, and Molecular Genetic Analysis of 10 Cases

Charles Leduc, William R Sukov, Jeannette G Rustin, Joseph J Maleszewski. Mayo Clinic, Rochester, MN.
Background: Angiosarcomas (AS) are the most common type of primary cardiac sarcoma with differentiation. Approved targeted therapies are lacking, and response to conventional therapies is suboptimal, leading to poor overall survival. Recurrent copy number variations and/or mutations have been identified in extracardiac AS, however these have yet to be investigated thoroughly in those arising primarily in the heart. This study aims to further define the molecular profile of cardiac AS, and correlate such with histopathologic features, clinical features, and course.
Design: Tissue registry archives at Mayo Clinic (Rochester, MN) were queried for cases of cardiac AS (1995-2014). Cases with sufficient tissue for molecular genetic testing were retained. Demographics and clinical follow-up were abstracted from the clinical record, histologic parameters were reviewed, and immunohistochemistry for cytokeratin AE1/AE3 and vascular markers (CD31, CD34, ERG, FLI-1) was performed. DNA was extracted from formalin-fixed paraffin-embedded tissue, and copy number and loss of heterozygosity analysis was carried out with a whole genome single nucleotide polymorphism-based platform (OncoScan).
Results: 15 cases were identified, 10 of which had sufficient tissue for molecular testing. Mean age was 47.3 years, male:female ratio was 1.5:1, and median survival was 5.2 months (1-60 mos). There was no thoracic irradiation in the cohort. The majority (7/10) occurred in the right atrium, and average size was 6.3 cm (2.5-9.8). All cases had necrosis and the mean mitotic count was 13/10 hpf. 13 cases had spindle cell morphology, 1 epithelioid and 1 mixed. ERG was the most sensitive vascular marker (diffuse in all cases), and 4/10 cases were at least focally positive for CK AE1/AE3. The most common genetic alteration was polysomy 8 (n=8), followed by polysomy 4 (n=4) and gain of 1q (n=4). In no cases was there specific amplification of *MYC* (8q24). Gain of 1q was accompanied by polysomy 8 in all 4 cases, and was associated with a trend towards longer survival compared to cases without gain of 1q (31.8 vs 4.4 mos, p=0.065, Log Rank).
Conclusions: This is the first study to have comprehensively studied cardiac AS form a molecular standpoint. Recurrent chromosomal aberrations were identified and include polysomy 8, polysomy 4, and gain 1q. The lack of *MYC* amplification is in keeping with the strong association of this aberration with radiation. While the mechanism remains unclear, our data shows that 1q gain may be associated with prolonged survival, which suggests possible prognostic role of molecular testing in cardiac AS.

326 How to Choose the Pathologic Marker of Evaluate the Irreversibility of Congenital Heart Disease Associated Pulmonary Hyptertension

Li Li, Changming Xiong, Shian Huang, Chao Liu, Hongyue Wang, Xuejing Duan, Jianguo He. Fuwai Hospital, National Center for Cardiovascular Diseases, Chinese Academy of Medical Sciences, Peking Union Medical College, Beijing, China; Guangdong Medical College Affiliated Zhanjiang Hospital, Zhanjiang, China; Gaozhou People's Hospital, Gaozhou, China.
Background: This study sought to assess the pathologic markers to evaluate the irreversibility of congenital heart disease associated pulmonary hypertension (CHD-PAH).
Design: Tweenty-eight patients with CHD-PAH were divided into two subgroups of reversible pulmonary hypertension (RPAH) and irreversible pulmonary hypertension (IPAH) according to postoperative mean pulmonry artery pressure (MPAP). Pulmonary vascular lesion was analyzed according to Wagenvoort's methods. Mean medium thickness percent (%MT), mean medium area percent (%MA) and pulmonary arteriole density were measured by quantitative morphometric techniques. The immuonactivities of transgelin and filamin A were analyzed by immunohistochemistry.
Results: Of all 28 patients, 24 were RPAH and 4 were IPAH. Of all 24 patients with RPAH, 13 biopsies (54.2%, 13/24) had pulmonary vascular lesion of grade 0, 9 (37.5%, 9/24) with grade 1 and 2 (8.3%, 2/24) with grade 2. Of 4 IPAH, 1 biopsy had lesion of (25%, 1/4) grade 1, 1(25%, 1/4) with grade 2 and 2 (50%, 2/4) with grade 3. Both preoperative and postoperative MPAP were higher in IPAH patients than that in RPAH patients (53.3±23.4mmHg vs 34.1±12.7mmHg, p=0.020 and 35.0±8.8mmHg vs 17.8±3.9mmHg, p<0.001). Compared to those patients with pulmonary vascular lesion of grade 0 and 1, the preoperative MPAP in the patients with grade 2 and 3 had no significant difference, but the postoperative MPAP was higher ($p<0.05$ *or* 0.01). Compared to control group, %MT and %MA were significantly increased in RPAH and IPAH group (12.0±3.5, 8.5±2.0 vs 5.7±1.0, p<0.001 and 55.8±11.1, 49.0±9.4 vs 34.0±5.5, p<0.001). Correlation analysis demonstrated that %MT and %MA had positive correlation to preoperative and postoperative MPAP. Transgelin and filamin A had stronger immunoactivitis in pulmonary vascular smooth muscle cells in IPAH than that in RPAH and control group.
Conclusions: Pathological diagnosis of lung biopsy was still the golden criterion to evaluate the irreversibilty of PAH. Mean medium thickness percent, mean medium area and immunoactivities of transgelin and filamin A was helpful to evaluation the irreversibilty of PAH.

327 Characterization of LVAD Ventricular and Aortic Interfaces: Potential Role in Device Thrombosis

Daniel Pelletier, Stanley J Radio. University of Nebraska Medical Center, Omaha, NE.
Background: Left ventricular assist devices (LVAD) have become increasingly common therapy for heart failure patients as a bridge to transplant or destination therapy. Thromboembolic events are a significant cause of device failure, morbidity, and mortality. Limited information exists on the healing of LVAD connections with native hearts, and their contribution to thrombus formation.
Design: Explant and autopsy specimen LVADs from 65 patients (M=52, F=13, ages 20-75 yrs, ave=54.8 yrs) with implant duration between 2 weeks-22 months were available for review. For each specimen, the length and % circumference of LV cannula fibrous ongrowth (FG) exterior and interior, presence and degree of luminal obstruction, aortic graft neointima length and % circumference, and presence of thrombus (inflow/outflow cannula, device housing) were recorded. Histologic exam was performed on each device interface.
Results: FG was present on 100% of exterior LV cannulae, ranging from 3-20 mm (avg 12). FG cannula circumference was over 50% in 83.1% of specimens. FG on the LV cannula lumen ranged from 1 to 15 mm (avg 5.1), with 85.2% of specimens displaying some degree of luminal FG. Luminal obstruction by FG was present in 43.1% of specimens. 31% of specimens had obstruction between 1-10% of luminal area, with 8.6 and 3.4% of specimens displaying 11-25% and 26-50% obstruction, respectively.
Neointima of the aortic graft was present in 93.5% of explants and ranged from 1-20 mm (avg 8.4) and involved >50% of the circumference in 58.7% of devices. Intimal reaction of the native aorta was present in 31%, and ranged from 1-8 mm (avg 2.8) with 12.5% involving >50% of the circumference.
Thrombus was present in the LVAD pump of 24.5% of specimens, ventricular cannula outlet in 1.64%, and aortic graft outlet in 12.2%.
The healing reaction at the LV cannula/LV site consisted of chronic inflammation (lymphocytes, histiocytes, foreign body giant cells, and plasma cells) and granulation tissue with variable degrees of fibrosis. The neointima at the aortic anastomosis consisted of collagen or fibromyxomatous matrix with smooth muscle cells lined by endothelial cells.
Conclusions: Fibrous ongrowth was present in all patients and tended to increase with implant duration. Such ongrowth led to at least some luminal obstruction in 43%, including greater than 25% luminal area obstruction in 2 devices. Thrombus was present at various locations in 26% of patients. In our study, 47% of patients with thrombus had some degree of LV cannula luminal obstruction, suggesting it may play a role in the development of thrombus.

328 Sudden Cardiac Death in Young Athletes: Are There Gender Differences in the Cause of Death?

Kalliopi Pilichou, Stefania Rizzo, Elisa Carturan, Marialuisa Valente, Gaetano Thiene, Cristina Basso. University of Padua, Padua, Italy.

Background: No specific data are available on the prevalence and characteristics of cardiac sudden death (SCD) during sport activities among young women.

Design: Prospective target project on SCD in the young (1-40 years old), including clinical charts review when available and circumstances of death collection. SCD investigation performed according to the European guidelines with gross, histology and molecular investigation, when deemed necessary.

Results: Among 695 subjects 1-40 years old who died suddenly in the same geographic areas, 649 were due to SCD (196 female, 30%). A total of 76 young adults were competitive athletes and died during or soon after effort (11%). Only 6 (8%) of such events occurred in women (mean age 23±10 yrs, range 12-38), specifically during jogging (2), and swimming, volley, gymnastic and triathlon (one each).

Cause of death seemed more likely to be associated with structurally normal heart in women compared with men (50% versus 7%; P<0.01). In particular, while inherited cardiomyopathies (i.e. arrhythmogenic, hypertrophic and dilated) and coronary atherosclerosis are the leading cause in the overall population of athletes (24/76, 32% and 11/76, 14.5% respectively) and in the male sub-group (24/70, 34% and 11/70, 16%, respectively), they were never observed in female athletes.

Conclusions: Sports-related SCD in women is dramatically less common compared with men. In the female athletic population, SCD occurs in the setting of a structurally normal heart in half of cases. In a country with obligatory pre-participation screening for sport activity, inherited cardiomyopathies and atherosclerotic coronary artery diseases are almost exclusive of the male athletic population

329 Morphologic and Genetic Features of Arrhythmogenic Cardiomyopathy: Are There Differences between Sudden Death and Cardiac Transplantation Cases?

Kalliopi Pilichou, Stefania Rizzo, Elisabetta Lazzarini, Elisa Carturan, Marco Cason, Rudy Celeghin, Annalisa Angelini, Marialuisa Valente, Gaetano Thiene, Cristina Basso. University of Padua, Padua, Italy.

Background: Arrhythmogenic cardiomyopathy (AC) is an autosomal dominant heart muscle disorder characterized by a progressive fibro-fatty replacement of myocardium, accounting for life-threatening arrhythmias, sudden death (SD) and more rarely heart failure. Although nearly half of AC patients harbor mutations in genes encoding desmosomal components, nucleotide variations in other cardiac-related genes by massive parallel sequencing have been recently described, suggesting a more complex genetic background.

Design: Heart specimens of AC patients from either cardiac transplantation (CT) (A) or SD (B) underwent gross and histologic evaluation. Genetic screening was carried out in all for 150 cardiac-related genes (Nextera custom panel, MiSeq, Illumina). Pathogenicity of nucleotide variations was determined through in silico prediction algorithms as well as filtering in exome variant server, dbSNP, HGMD, ClinVar, ARVC/D database.

Results: Pathology study: A) Among 17 CT cases (13-70y), 14 (82%) had the classical AC variant with wall thinning, RV aneurysms at the inflow, apex, and outflow region, +/- left ventricular (LV) involvement. B) Among 28 SD cases (12-60y), 9 (32%) had the classical AC variant and 19 the LV dominant one with a subepicardial/midmural distribution. Histologically, myocardial atrophy with fibro-fatty replacement was confirmed in all.

Genetic screening: A) Of the 17 CT patients, 10 (59%) carried desmosomal gene mutations (4 PKP2, 7 DSP, 2 DSG2, 1 DSC2). All CT mutation carriers had a classical AC variant (10 of 14, 70%), 6 of whom carrying a radical mutation (nonsense/frameshift either in homozygosis or in single/compound heterozygosis), and 4 carrying a missense mutation (of whom 1 homozygote and 1 compound heterozygote). The remaining 8 CT cases harbored desmin (2), SCN5a (1) and MyBPC3 (2) mutations. B) Of the 28 SD cases, 11 (39%) carried desmosomal gene mutations (6 PKP2, 4 DSP, 1 DSG2, 1 DSC2). Noteworthy, desmosomal mutations were found in 7 (78%) of the 9 classical AC cases (7 radical and 1 missense), but only in four (24%) of the 17 LV dominant cases (4 missense and 1 radical). Among the remaining 15 SD victims, rare nucleotide variations in desmin (1) and MyBPC3(2) were found, all cases with a LV form.

Conclusions: More than 70% of classical AC variants are associated with desmosomal gene mutations. A wider genetic spectrum is found in the dominant LV variants, with higher prevalence of nondesmosomal mutations suggesting a more complex inheritance pattern of AC than previously appreciated.

330 Sudden Cardiac Death with Structurally Normal Heart: ECG Tracing and Molecular Autopsy as a Guide for Conduction System Investigation

Kalliopi Pilichou, Federico Migliore, Marco Cason, Stefania Rizzo, Rudy Celeghin, Emanuele Bertaglia, Elisabetta Lazzarini, Elisa Carturan, Marialuisa Valente, Gaetano Thiene, Cristina Basso. University of Padua, Padua, Italy.

Background: Sudden cardiac death (SCD) with normal heart can occur in the setting of inherited ion channel diseases. Among these, Lenégre disease (progressive atrio-ventricular block) is characterized by structural changes of the conduction system and mutations in the α subunit of the cardiac sodium channel (SCN5A).

Design: Autopsy with gross and histologic examination of the heart of the index case was carried out including molecular autopsy through screening a panel of 150 cardiac-related genes (Nextera custom panel, MiSeq, Illumina). Mutation pathogenicity was determined by in silico prediction algorithms and filtering in exome variant server, dbSNP, HGMD, ClinVar, LOVD database. Detailed conduction system investigation by serial section technique was performed guided by ECG and genetic findings. Cascade genetic screening of family members with clinical investigation in mutation carriers.

Results: A 35-years old asymptomatic male died suddenly during sleep. Post-mortem examination excluded extracardiac causes of SCD as well as the absence of structural abnormalities in the working myocardium. Personal clinical history re-assessment revealed a 'coved-type' ST segment elevation on right precordial leads with PQ prolongation (220 msec) in a patient's ECG performed during blood donation, compatible with Lenégre disease. Genetic screening identified a mutation in exon 22 (c.3673 G>A, E1225K) of SCN5A (NM. 198056.2) gene, defined as "likely to be pathogenic" by in silico tools and linked to progressive atrio-ventricular block. Detailed conduction system investigation showed severe fibrosis of the bifurcating His and proximal bundles with sclerotic interruption of the left bundle branch. Cascade genetic screening detected 5 additional family mutation carriers, and provoked electrical stimulation unmasked ECG abnormalities in 2 of them.

Conclusions: Conduction system investigation is rarely performed in SCD due to difficult interpretation of histologic findings in the absence of clinical data. Conduction abnormalities on ECG and positive molecular autopsy are of help in selecting cases to be investigated by serial section technique.

331 Myocardial Capillary Density in Left and Right Ventricles of Explanted Hearts from Patients after Short and Long Term Heart Transplantation

Jihui J Qiu, Theodore Vasiliadis, Xu Wang, Jieliang Li, Xulei Liu, Nirag C Jhala, He Wang. Temple University Hospital, Philadelphia, PA; Vanderbilt University, Nashville, TN.

Background: Pathological analysis of left ventricular capillary density (CD) after heart transplantation, as well as the relationship of CD with left ventricular function, is lacking. Rare data using right ventricular endomyocardial biopsies suggest capillary rarefaction after heart transplant.

Design: We analyzed the relationship between myocardial CD and the duration of implantation using ventricular tissue generously obtained from explanted hearts at autopsy. The retrospective analysis involved 20 subjects including 14 orthotopic heart transplantation (OHT) subjects and 6 control subjects without OHT. Subjects with OHT were divided into short-term (within 6 months after OHT, n=4) and long-term groups (more than 6 years after OHT, n=10). CD was evaluated after CD31 staining, while ventricular fibrosis was analyzed after trichrome staining, using ImageJ software for the quantitative morphometric analysis. mRNA levels of vascular endothelial growth factor (VEGF) and basic fibroblast growth factor (bFGF) in ventricular tissue were measured by quantitative reverse transcription polymerase chain reaction.

Results: CDs of left ventricles were significantly higher in the short-term group compared to the control group (1773+/- 232 versus1007 +/- 390 capillaries/mm^2; P=0.008) or the long-term group (1773+/- 232 versus 1150 +/- 389 capillaries/mm^2; P=0.010). No significant difference in CD was found between long-term and control groups. The changes of right ventricular CD showed a similar trend. There was no significant change of VEGF or bFGF mRNA levels in ventricular tissue between control, short-term and long-term groups. There was a significant increase in fibrosis of ventricular tissue in the long-term group compared to the control group (median [interquartile range (IQR)] = 5.51 [3.70, 15.43] versus 2.12 [1.45, 2.18] %, P = 0.0043). No significant difference in fibrosis was found between short-term and control groups. There was no significant correlation between left ventricular CD, left anterior descending coronary artery (LAD) lesion and ventricular fibrosis.

Conclusions: Our study revealed a significant increase in CD of left and right ventricles in transplanted hearts within 6 months after OHT; CD decreased thereafter to the levels in hearts without OHT. The mechanism of the early angiogenesis is under further investigation. No direct correlation between myocardial CD, LAD lesion and ventricular fibrosis was identified.

332 Transcathether Ablation of the Atrio-Ventricular Junction: Histopathology Findings and Interventional Anatomy of the Tricuspid Valve

Stefania Rizzo, Andrea Corrado, Franco Zoppo, Marialuisa Valente, Gaetano Thiene, Cristina Basso. University of Padua, Padova, Italy; Mirano Hospital, Mirano, Italy; Mestre Hospital, Mestre, Italy.

Background: Catheter ablation of the Atrio-ventricular junction (AVJ) followed by pacemaker implantation is used for atrial fibrillation therapy. The endocardial approach can be either from the right side or more rarely from the left side. Data about the ideal interventional anatomy of the tricuspid valve (TV) and the histologic features after successful ablation are missing.

Design: A total of 100 human hearts were examined for the anatomic variability of the continuity between the anterior and septal TV leaflets. Hearts form patients with successful catheter abaltion of AVJ were studied by serial section techniques of the conduction system.

Results: In 98% of cases, a continuity between the anterior and septal TV leaflets was found (3.8±2.9 mm). Four patients with atrial fibrillation had a previously successful catheter ablation.Tthree of them had a TV leaflets continuity. Ablation from the right side was successful in all except one requiring a left side approach. Conduction system investigation revealed fibrosis of the AV node and/or His bundle in each case with a right side approach, while extensive fibrosis of the ventricular septum crest and branching bundle but an intact AV node were observed in the setting of a left side approach.

Conclusions: The anatomic variability of the antero-septal commissure of the TV can affect a successful AVJ ablation, since the continuity protects the AV node from ablation with a right side approach. In this setting, multiple shocks are required, seldom necessitating a switch to a left side approach.

333 Erosion Is More Common as a Cause of AMI in the Elderly: A Pathologic Study of Coronary Arteries in 884 Human Autopsy Cases

Atsuko Seki, Koji Chida, Akihiko Hamamatsu, Motoji Sawabe, Yoko Matsuda, Keisuke Nonaka, Shinichiro Ohkawa, Tomio Arai. Tokyo Metropolitan Geriatric Hospital, Itabashi, Tokyo, Japan; Kasumigaseki Clinic, Chiyoda, Tokyo, Japan.

Background: The most common cause of AMI is believed to be the rupture of thin cap fibroatheroma (TCFA). Few data are available regarding the cause of AMI in the elderly. We hypothesized that a different mechanism was operative.

Design: Formalin-fixed human coronary arteries from 884 patients (mean 81.2 yrs, 55.5% men) were serially examined at 5 mm intervals. Of those, 6.1% of patients had AMI (n=54). Cases with previous cardiac intervention (PCI/CABG) and OMI (n=97) were excluded. The culprit lesions were paraffin embedded, serially cut into 5-μm-thick sections, and stained with H&E, EVG, and Azan (46,111 sections). Twenty-four culprit plaques (LAD, n=11; LCX, n=6; RCA, n=7) were classified as erosion, rupture of TCFA (<65 μm), calcified nodule (calcified plaque with eruptive calcified nodules), or stenosis without eruptive calcified nodules or thrombi. Micro-Computed morphometry was used to characterize plaques.

Results: Erosion was the most common cause of AMI (54.2%; mean, 85.0 yr). Plaque rupture of TCFA was found in 16.7% (mean, 77.3 yr) of culprit lesions (table 1); calcified nodule in 16.7% (mean, 90.0 yr), and stenosis in 12.5% (mean, 86.7 yr).

mean (range)	Erosion (n=13)	Rupture of TCFA (n=4)	Calcified nodule (n=4)	Stenosis w/o thrombi (n=3)
Female/Male	8/5	1/3	2/2	1/2
Age (yr)	85.1 (72-95)	77.3 (65-92)	90.0 (79-104)	86.7 (80-96)
Actual luminal area decrease (%)	95.9 (83.1-99.7)	89.2 (79.3-95.9)	94.8 (93.8-96.9)	98.6 (97.4-100)
Necrotic core (%)	41.0 (8.8-82.8)	45.0 (16.6-64.5)	11.8 (n=1)	56.2 (52.6, 59.8; n=2)
Collagen-rich area (%)	55.2 (16.2-86.2)	55.6 (34.6-85.0)	70.2 (36.1-99.1)	59.5 (37.4-94.6)
Calcifications (%)	11.5 (0.3-44.8)	5.4 (2.0-8.6; n=3)	15.9 (9.3-21.2)	7.4 (5.7, 9.1; n=2)
Intraplaque hemorrhage (%)	7.6 (0.4-28.4)	15.2 (0.3-31.7)	14.3 (1.9-29.1)	10.6 (3.2-21.2)
Minimum fibrous cap thickness (μm)	247.3 (21.5-792.2)	17.9 (10.0-23.4)	n=0	231.0 (101.9, 360.1; n=2)

Stenosis was severe in all groups; erosion (mean, 95.9%), calcified nodule (mean, 94.8%), rupture (mean, 89.2%), and stenosis (mean, 98.6%). TCFA was found in all rupture cases and one erosion case.

Conclusions: Erosion was the most common culprit lesion in fatal AMI in the elderly. TCFA was present in only 20.8% of the culprit plaques. The different pathogenesis of AMI in the elderly suggests that other strategies might be necessary to prevent AMI in this age group.

334 C4d-Negative, DSA Positive Antibody-Mediated Rejection in Heart Allografts

Kelly Smith, Karen Nelson. University of Washington, Seattle, WA; BloodWorks Northwest, Seattle, WA.

Background: Antibody-mediated rejection (AMR) is a challenging clinical and pathologic diagnosis. Recently, within the renal transplant community, microvascular inflammation has emerged as a sensitive marker of AMR, and uncovered the existence of C4d- DSA+ AMR. The diagnostic criteria for C4d-negative antibody-mediated rejection in heart allografts has not been established. We evaluated the clinical, pathologic and laboratory data for for 122 allografts performed at our institution, in order to determine criteria to define AMR.

Design: We reviewed pathology, laboratory and clinical data for 122 orthotropic heart transplant cases done between September 2008 and September 2014. These patients had undergone 563 biopsies, 346 immunopathologic studies and 703 DSA assays, using single antigen bead technology.

Results: Out of 346 immunostains for C4d, we had 44 (13%) C4d+ biopsies. 25 (57%) C4d+ biopsies were from DSA+ patients. 47 (63%) of 75 biopsies from DSA+ patients were C4d-, and 3 were indeterminate. 43% of C4d+ biopsies were from DSA- patients. Out of 563 biopsies we had 30 (5.3%) biopsies with histologic findings suggestive of antibody mediated rejection (H+). 15 (50%) H+ biopsies were from DSA+ patients and 15 (50%) H+ biopsies were from DSA- patients. We had 3 (0.86%) biopsies that were H+ and C4d+, and all of these were from DSA+ patients.

Conclusions: The majority of DSA+ patients have C4d negative biopsies. C4d-, DSA+ biopsies may represent: a prelude to C4d+ AMR, successful treatment of C4d+ AMR, subclinical AMR, or clinically relevant AMR. Future studies are needed to define histologic/immunopathologic features or other tests that will help diagnose clinically relevant C4d- AMR.

335 Biochemical Signature of Antibody-Mediated Rejection in Cardiac Allograft Biopsies

Imran Uraizee, Michael Walsh, Peter Nguyen, Aliya N Husain. University of Chicago, Chicago, IL; University of Illinois at Chicago, Chicago, IL.

Background: Antibody-mediated rejection (AMR) in cardiac allograft recipients remains less well-understood than acute cellular rejection, is associated with worse outcomes, and portends a greater risk of developing chronic allograft vasculopathy. Diffuse immunohistochemical (IHC) complement 4d (C4d) staining of capillary endothelia in formalin-fixed, paraffin-embedded (FFPE) right ventricular (RV) endomyocardial biopsies is the current gold standard for diagnosis of immunopathologic AMR but serves only as a late-stage marker. Label-free biochemical imaging by infrared (IR) spectroscopy of FFPE RV tissue may facilitate identification of a unique biochemical signature of AMR.

Design: From 23 FFPE RV tissue biopsies obtained during cardiac allograft rejection surveillance (11 negative for any type of rejection, 12 positive for immunopathologic AMR with diffuse IHC C4d endothelial staining), unstained 4mm sections were cut onto MirrIR low-e reflective slides for IR spectroscopic analysis. FFPE RV tissue biopsies from 11 native hearts without major diagnostic abnormality were also sectioned as a control group. IR absorption spectra of entire tissue sections were acquired and regions of interest (ROI) identified, including cardiomyocytes and endothelial cells. Extracted spectra were averaged across pixels within each ROI. Multivariate principal component analyses (PCA) were used to compare differences in absorption spectra among biopsies from each group. Linear discriminant analyses (LDA) were used to identify unique spectral classifiers.

Results: Comparison of IR spectra derived from cardiomyocytes and endothelial cells demonstrated unique spectral features between the C4d positive and negative biopsies. PCA demonstrated that the C4d positive and negative biopsies could be discriminated and visualized to separate into distinct groups. LDA yielded spectral classifiers permitting accurate automated classification of biopsies.

Conclusions: In cardiac allograft biopsies with immunopathologic AMR, IR spectroscopy reveals a biochemical signature unique to AMR compared to that of non-rejecting cardiac allografts and native hearts. Further work is ongoing to increase the number of patients and to determine whether a spectral signature preceding C4d deposition can predict later development of AMR.

336 Formalin Perfusion-Fixation of Autopsy Hearts for a More Accurate Evaluation of Coronary Artery Stenosis

Jonathan Vaucher, Justine Turmel-Roy, Olga Sazonova, Sylvain Page, Sylvain Trahan, Christian Couture, Philippe Joubert. Institut Universitaire de Cardiologie et de Pneumologie de Québec, Quebec, QC, Canada.

Background: Coronary angiography is the standard method for determining the site, extent and severity of coronary artery disease. Several publications have reported discordance between the degree of coronary artery stenosis as assessed by histologic evaluation when compared to angiography. Although angiography has inherent biases, histopathologic evaluation tends to overestimate the stenosis percentage owing to the relaxed state in which the coronary arteries are fixed and examined. The goals of this study were: 1) to achieve formalin fixation of hearts in conditions which simulate arterial systemic pressures by using a device of our own, 2) to determine if this method can reduce the overestimation of the degree of stenosis when compared to the passive immersion-fixation method.

Design: Autopsy hearts were fixed, either by passive immersion (n = 30) or by intra-aortic perfusion of formalin at 80-90 mmHg for at least 12 hours (n = 10). Coronary arteries were then dissected *en bloc*, serially sectioned and submitted for histology. Sections stained with Verhoeff von Gieson were digitized and the maximal percentage of stenosis was calculated by dividing the surface area of the residual lumen by the surface area delimited by the internal elastic lamina.

Results: The results are summarized in table 1. The mean percentages of stenosis for each coronary artery was significantly lower in the perfusion-fixation group than in the immersion-fixation control group.

Table 1 : Comparison between the mean percentage of stenosis of main coronary arteries in hearts fixed with a perfusion of formol versus hearts passively fixed

	Perfusion fixation (n=10)	Passive fixation (n=30)	P values
Mean age (years)	51.9	51.7	
LMA (% of MS)	30.9 ± 20.5	51.9 ± 20.6	0.01
LAD (% of MS)	46.1 ± 27.8	67.9 ± 19.1	0.04
LCX (% of MS)	41.2 ± 28.9	61.5 ± 19.9	0.06
RCA (% of MS)	37.9 ± 25.6	66.2 ± 21.8	0.01

Legend: LAD Left anterior descending artery; LCX Left circumflex artery; LMA Left main coronary artery; MS Maximal stenosis; RCA Right coronary artery. Values preceded by a ± character are standard deviations.

Conclusions: Our results suggest that perfusion-fixation reduces histopathological overestimation of stenosis severity compared to the passive fixation method. Further studies to evaluate which one of these two methods better correlates with the pre-mortem angiography are underway at our center.

337 Left Ventricular Assist Device Can Increase Capillary Density of Human Heart

Jindong Wang, Theodore Vasiliadis, Eman Hamad, Xu Wang, Viren Patel, Jieliang Li, Xulei Liu, Nirag Jhala, He Wang. Temple University Hospital, Philadelphia, PA; Vanderbilt University, Nashville, TN.

Background: Prolonged ventricular unloading with a left ventricular assist device (LVAD) or other continuous flow devices have been used significantly in recent years to treat severe heart failure. The use of LVAD has been shown to lead to myocardial recovery in some patients, indicating that some degree of cardiomyocyte regeneration can be induced by decreasing the external load. Furthermore, mitosis and cytokinesis were reported to increase significantly in the post-LVAD hearts. This study is aimed to determine the cellular response of human heart to the prolonged mechanical unloading by a LVAD.

Design: Pre- and post-LVAD heart tissue samples were collected from 11 patients at the time of LVAD implantation and heart transplantation. The 11 patients included 2 females and 9 males with age ranging from 27 to 71 and averaging 57. Four patients had ischemic cardiomyopathy and seven patients had non-ischemic cardiomyopathy. All had no histologic evidence of active myocarditis. The duration of LVAD ranged from 1.5 to 56 months with an average of 10 months. The tissue was processed in the histology lab of Temple University Hospital for H&E and immunostaining. The capillary density was measured by ImageJ software on the CD31 immunostained slides. The pre- and post-LVAD samples were compared using the Wilcoxon signed rank sum test. The mRNA levels of basic fibroblast growth factor (bFGF) were measured by quantitative RT-PCR from paraffin-embedded formalin-fixed tissue.

Results: Of the 11 matched pre- and post-LVAD tissue samples, 10 demonstrated an up to 167.1% increase in capillary density after the use of LVAD (range= 20.0-167.1%, 66.3+/49.5%). One showed a 30.1% decrease in capillary density (duration of LVAD=10 months). The increase of capillary density in post-LVAD cardiomyocytes is statistically significant (p=0.0098). The amount of changes in capillary density was not related to the duration of LVAD (p=0.69). There were no significant changes in the amount of bFGF mRNA between pre- and post-LVAD groups.

Conclusions: Significant positive effects on the vascular architecture of human heart were observed by the prolonged ventricular unloading of LVAD. This improved vascularization of cardiomyocyte may play a role in the switch from a hypertrophic state to a hyperplastic state induced by decreasing the external load of the human heart.

338 Diagnostic Value of T helper Type 17 (Th17) Cells in Moderate Acute Cellular Rejection of Cardiac Allograft

Yinong Wang, Leland B Baskin, Daniel G Fontaine, Shuhong Liu, Christopher Naugler. Calgary Laboratory Services, University of Calgary, Calgary, AB, Canada.

Background: A diagnosis of moderate acute cellular rejection (grade 2R) is clinically important since it triggers adjustment in the immunosuppressive regimen whereas mild acute cellular rejection (grade 1R) usually does not. However, myocyte damage, a required morphologic feature for diagnosis of grade 2R rejection can be difficult to ascertain since the morphologic spectrum of myocyte damage is wide and has subtle changes. Studies have shown a major source of discordance in the grading is the criteria used for the interpretation of myocyte damage. Thus, it is necessary to explore new ancillary studies such as immunohistochemistry to improve accuracy of the morphologic diagnosis of grade 2R rejection. Recent research data suggest that the IL-17 producing T helper type (Th17) cell plays a crucial role in the acute allograft rejection.

Design: 25 cases of cardiac transplant biopsies with moderate acute cellular rejection were found in archives of Calgary Laboratory Services. The immunohistochemical stain for IL-17 was performed on the paraffin sections of the above biopsy specimens. The previous cardiac biopsy with diagnosis of mild acute cellular rejection from the same patient with the moderate acute cellular rejection was used as control. The Th17 cells were counted in the lymphocytic infiltrate regions. The data are expressed as number of cells per high power field (HPF).

Results: As compared with mild acute cellular rejection, biopsies with moderate acute cellular rejection had significantly increased number of Th17 cells (2.99 ± 2.29 cells/HPF vs 1.14 ± 1.50 cells/PHF, $p<0.001$).

Conclusions: The Th17 cell infiltration in the cardiac allograft is associated with severity of cardiac acute cellular rejection. Evaluation the number of Th17 cells in the cardiac transplant biopsies might be helpful in assistance with diagnosis of moderate acute cellular rejection and improve diagnostic accuracy of moderate acute cellular rejection.

339 Beta Amyloid Precursor Protein in Carotid Artery Plaque Macrophages: Correlation with Features of Plaque Stability

Michael B Ward, Tyler A Jensen, Krishna Narra, Scott McNally, Dylan Miller. Intermountain Medical Center/ University of Utah School of Medicine, Salt Lake City, UT; University of Utah School of Medicine, Salt Lake City, UT.

Background: Beta amyloid precursor protein (bAPP) is the amyloidogenic protein present in amyloid deposits of Alzheimer plaques and cerebral amyloid angiopathy. Its native function and activity (when properly folded and not produced in excess) are not fully understood, however bAPP is found in platelets and has been implicated in vascular inflammation and atherosclerosis. The aim of this study was to determine whether native bAPP (not amyloid) could be found in carotid plaques and if its presence or localization correlated with features of plaque instability.

Design: Intact carotid endarterectomy specimens were obtained as part of an ongoing IRB approved radiology-pathology collaborative study. The samples were formalin fixed and decalcified. H&E and elastic stains were performed to allow for characterization of plaques and features of instability (soft/necrotic atheroma, intraplaque hemorrhage, thin fibrous cap, cap inflammation). Immunoperoxidase staining for bAPP (DAKO clone 6F/3D) was also performed and the stained sections reviewed. The localization of staining was recorded along with a semiquantitative assessment of staining intensity and abundance. Immunohistochemistry data was correlated with features of plaque instability using the Pearson correlation method.

Results: 55 carotid tissue blocks from 35 patients comprised the sample population. The mean patient age was 69 years and 3 were women. 12 had ipsilateral strokes. 35 (64%) of the plaques showed features of instability. bAPP staining was limited to macrophages in a coarse granular cytoplasmic pattern, consistent with the reported phenomenon of macrophage phagocytosis of platelets expressing bAPP. These cells were present in and around the plaque cap and in areas of plaque hemorrhage. For unstable plaques, the mean semiquantitative bAPP score was 1.9 and for stable plaques it was 0.6 ($p<0.0001$) Correlation coefficients were determined for semiquantitative bAPP scoring versus percent of soft/necrotic plaque component ($r=0.57$, $p<0.0001$), thickness of fibrous cap ($r=0.14$, $p=.31$), and cap inflammation ($r=0.34$, $p=0.012$).

Conclusions: This preliminary study is the first to show accumulation of non-amyloid bAPP within carotid plaques and demonstrate an association with at least some specific features of plaque instability. Whether bAPP accumulation has mechanistic significance beyond plaque inflammation and instability remains to be determined and needs further study.

340 Implementation of the New AECVP/SCVP Aorta Consensus Grading Scheme

Kevin Waters, Andrew Guajardo, Marc K Halushka. Johns Hopkins University SOM, Baltimore, MD.

Background: The Association for European Cardiovascular Pathology (AECVP) and the Society for Cardiovascular Pathology (SCVP) have developed a new consensus nomenclature and grading scheme for degenerative, noninflammatory thoracic aortic specimens in order to improve the consistency of diagnosis for this specimen type. We tested the usability of these new terms on routine surgical pathology aorta cases.

Design: 100 consecutive noninflammatory aortic specimens and basic phenotypic data were obtained from the surgical archives. After an initial general review of aortic histopathology with two trainees and one cardiovascular pathologist, each case was independently scored by two observers in a blinded fashion for 13 features using H&E and Movat stained slides. All data was categorized, converted into numbers, tabulated and analyzed using a Mann Whitney U test.

Results: There was strong overall consensus on the overarching diagnosis of medial degeneration with only 3 of 100 cases demonstrating two levels of disagreement. There was more variability in the usage of less common findings such as elastic fiber thinning. Forty-seven cases had a known genetic syndrome (bicuspid aortic valve (BAV), Marfan, Loeys Dietz, FTAAD), with an average age of 42. The average age of the non-syndromic cases was 63. There was significantly less overall medial degeneration in subjects with BAV (n=31) than in the other syndromic cases ($p=2.2x10^{-3}$). Among the non-syndromic cases, overall medial degeneration increased with age. This was the result of increasing amounts of smooth muscle cell nuclear loss, laminar medial collapse and mucoid extracellular matrix accumulation (MEMA).

Conclusions: The new AECVP/SCVP Aorta Consensus Grading Scheme is a robust method for general surgical pathology signout and research studies. New, less common terminology will require increasing familiarity for consistent implementation. A new uniformity between centers can now be accomplished. Even within a small study set, we uncovered significant differences associated with syndromes and aging. With increasing use and larger study sets, it may now be possible to associate histopathologic findings with specific syndromes and increase the value of the surgical thoracic aorta.

Cytopathology

341 Can the Ki-67 Index Evaluated on Fine Needle Aspiration Cellblock Material Reliably Grade Pancreatic Neuroendocrine Tumors?

Rita Abi Raad, Andrea L Barbieri, Xuchen Zhang, Malini Harigopal, Rebecca Baldassarri, Angelique W Levi, Susan V Fernandez, Diane Kowalski, Adebowale Adeniran, Guoping Cai. Yale School of Medicine, Nerw Haven, CT.

Background: Currently, the best predictor of pancreatic neuroendocrine tumor (PNET) behavior is the tumor grade determined by measuring mitotic activity or/and Ki-67 index on surgically resected specimens. Although fine needle aspiration (FNA) is widely used in the preoperative diagnosis of PNETs, its role in prognostic evaluation of the tumors is very limited. The goal of this study was to assess the tumor grade, as determined by the Ki-67 index, on FNA cellblock material and correlate with the final grade on resection specimens.

Design: The institutional pathology database was searched for PNETs diagnosed by FNA between January 2006 and August 2015. Only the cases with available cellblock material and corresponding surgical specimens were included in the study. Clinicopathologic characteristics, cytological and surgical follow-up cases were retrospectively reviewed. The cytological diagnosis of PNETs was rendered by cytomorphologic analysis and adjunctive chromogranin and synaptophysin immunostains. Surgically resected tumors were graded according to 2010 WHO classification and staged following 2010 AJCC staging criteria. Ki-67 immunostain was retrospectively performed on FNA cellblocks and resected tumors if not performed initially.

Results: A total of 48 FNA cases with corresponding resections were identified. The cellblock sections contained >1000, 500-1000, 250-500, 100-250, and <100 tumor cells in 23, 9, 10, 2 and 4 cases, respectively. The resected tumors ranged from 0.9 to 8.5 cm (mean = 3.2 cm) and were graded as G1 and G2 tumors in 24 and 24 cases, respectively. In G1 tumors, the Ki-67 grading based on cellblock sections showed a 100% correlation rate with the grading on surgical specimens, regardless of cellblock cellularity and tumor size. However, in G2 tumors the correlation rate between cellblocks and surgical